Dhaka Univ. J. Sci. 69(1): 53-57, 2021 (January)

Electronic Properties and Scanning Tunneling Microscopy Simulation of MoS_2 Nanosheets by Using Density Functional Theory

Fariha Ahmed and Alamgir Kabir*

Department of Physics, University of Dhaka, Dhaka 1000, Bangladesh

(Received : 1 December 2020; Accepted : 24 February 2021)

Abstract

The ab-initio Density Functional Theory (DFT) approach is used to study the electronic properties of bulk and layered MoS_2 nanosheets. For the layered structures mono, bi, tri, tetra and penta layered structure is used. The direct to indirect transition of bandgap is observed as the number of layers is increasing. This transition of bandgap is attributed to the van der Waals interlayer interaction between two layers of MoS_2 nanosheets. The indirect bandgap in the bulk MoS_2 is found to be 0.94 eV, whereas for a single layered nanosheet is found to be direct bandgap with the value of 1.83 eV. To confirm the surface termination and understand the surface morphology of MoS_2 the scanning tunneling microscopy (STM) simulation is performed in constant height mode. It is found that the detection of surface atoms via STM depends on the tip atom of the STM.

Keywords: Bandgap, van der Waal's, catalysis, STM tip, indirect bandgap

I. Introduction

Layered transition-metal dichalcogenide (TMDC) nanosheets have attracted attention due to their potential application in nano electronic devices,[1] spintronics,[2] optoelectronic devices, catalyst[3], effective solid lubricant[4], and electrochemical sensors.[5–8] Amongst the TMDCs, molybdenum disulfide (MoS_2) is very cheap and easily available. In a bulk MoS_2 hundreds of single layers are stack together with van der Waal's force. Since van der Waal force is very weak, to separate a single layer from a bulk sample of MoS_2 is very easy. Each layer of MoS_2 has a plane of hexagonally arranged Mo atoms sandwiched between two planes of hexagonally arranged S atoms, with the covalently bonded S-Mo-S atoms in a trigonal arrangement forming a hexagonal crystal structure. The theoretical formation of a single layer MoS_2 from its bulk structure is rather easy which can be created by deleting some of the adjacent layers.[9]

Electronic properties change drastically when MoS_2 is reduced from bulk to a single layer. [10] The MoS_2 monolayer has unique mechanical, electrical, optical and chemical properties.[10] This uniqueness of single layered MoS_2 make it very useful in practical applications, and the morphology of a layer is very important for practical device fabrications.[11] It has been suggested that the electronic properties of MoS_2 have a strong dependence on the number and distance of planes composing the system. Based on this transition from direct to indirect bandgap, a single layer MoS_2 was used to construct a transistor. The direct bandgap monolayer also demonstrates strong photoluminescence as a result of quantum confinement.[12]

It was found in the scanning tunneling microscopy (STM) experiment by Tianshu Li and Giulia Galli that the morphology and electronic properties of MoS_2 nano flacks depends on the size of the flacks.[13] The size and the morphology of the nanoparticles was found to have strong dependence on the nature of surface atoms of the nanoparticles. The nanoparticles with large number of S atoms on the surface has much profoundness than the Mo atoms on the surface of the nanoparticles, which indicate that the S covered nanoparticles are energetically more favorable than the Mo covered one.

To understand the electronic and morphological properties of MoS_2 nanolayers, we have carried out systematic electronic structure calculations. The ab initio density functional theory (DFT) is used for the simulation of electronic structures. The most widely used method for theoretical calculations is DFT since it considers the quantum mechanical interaction of the electron and ions of the materials into account. In DFT formalism the electronic density of the materials is considered to be the source of all physical and chemical properties of a material rather the position and number of electrons. A detailed theoretical study of single-layer and multi-layer structures MoS_2 nanosheet is also performed in this work. The scanning tunneling microscope (STM) images can be obtained from the density of states (DOS) of the surface atoms of the semiconducting materials. We have used the Tersoff-Hammen approximation[14] to study the surface morphology of the MoS_2 surface

II. Computational Details

The DFT approximation as implemented in the Viena Ab-initio Simulation Package (VASP)[15] is used to carry out all the calculations. The electronic exchange and correlation effects are included by Perdew-Burke-Ernzerhof (PBE) pseudo potential which uses the generalized gradient approximation (GGA)[16]. The Projected Augmented Wave (PAW) technique was used to describe ion-electron interactions. The effect of van der Waals interactions is included by using the D3 correction scheme of Grimme *et al* with Becke-Jonson damping. The cut off energy for the plane wave basis was set as 600 eV. The Gamma centered k-sampling is used as KPOINTS and the 12x12x12 k-points are used for the bulk calculations. For the layered MoS_2 we have used 12x12x1 k-points mesh since the layers are infinite in x and y directions and finite in z direction. For the nanoparticles only a single k-point centered at gamma point in the Brillouin zone is used. Visualization for Electronic and Structural Analysis (VESTA) software was

*Author for correspondence. e-mail: *alamgir.kabir@du.ac.bd*

used to model the initial structures. For modeling of the layered structures, a gap of 6 Å is included along the z-direction both on the upper and lower side of the layer, so that a layer cannot have Coulombic interaction between its periodic images. Conjugate gradient algorithm is used for ionic relaxation and the ions are allowed to move freely in all three directions in space. The force convergence criterion was set to 0.01 eV/Å.

III. Results and Discussion

Bulk and Layered MoS_2 nanosheets

MoS_2 is a layered 2D material and there is van der Waals interaction exist between two adjacent layers. The unit cell of MoS_2 consist of two layers of S-Mo-S. The optimized bulk structure of MoS_2 is shown in the Fig 1(a), it has structural symmetry of $P6_3/mmc$ with a layer staking 2Hc type. The hexagonal lattice constant is obtained to be 3.20 Å, the height of a single S-Mo-S layer is 3.16 Å, and the separation between two adjacent S-Mo-S layers is found to be 3.00 Å. These values are in good agreement with the experimental values obtained by T. Boker et al[17] and with other DFT calculation[18].

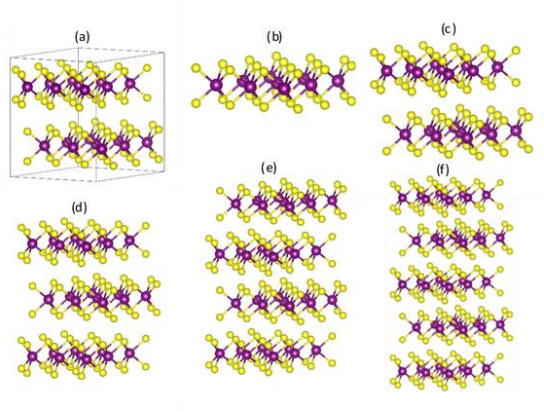

Fig. 1. (a) Bulk, (b) Monolayer, (c) Bi layer, (d) Tri layer, (e) Tetra layer, and (f) Penta layer of MoS_2 nanosheet. Mo atoms are indicated by purple(black) balls and S atoms are indicated by yellow (white) balls.

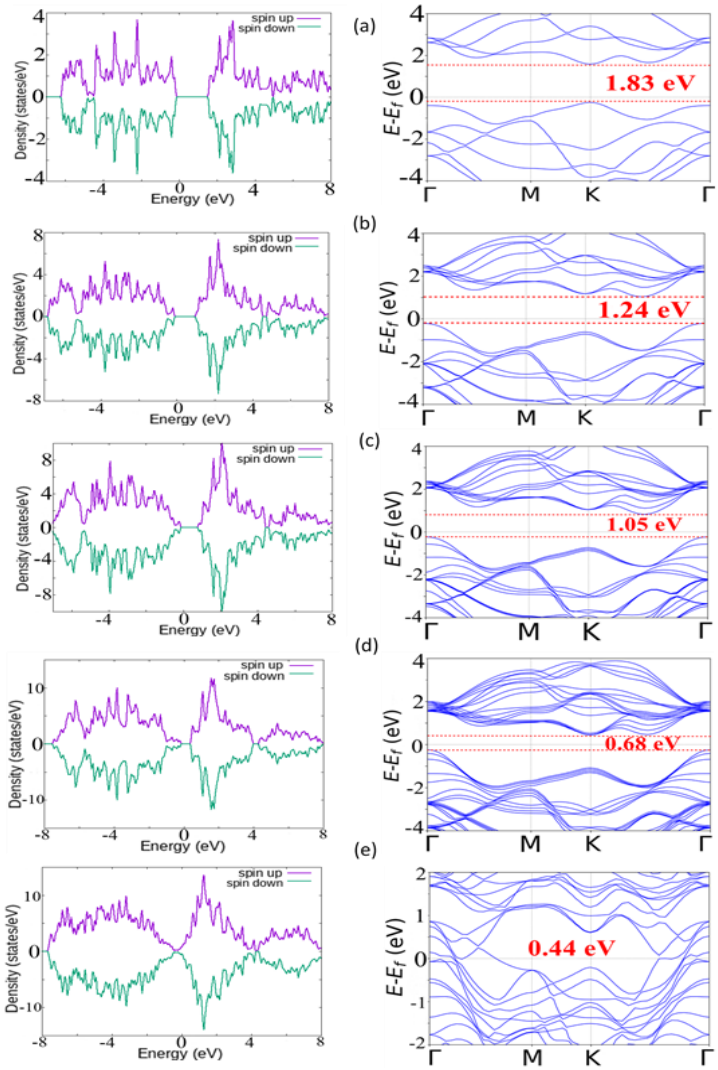

Fig. 2. Left panel represents the DOS and right panel represents the band structures of (a) mono-layer, (b) bi-layer, (c) tri-layer, (d) tetra-layer, and (e) penta-layered MoS_2 nanosheet, respectively.

The monolayer, bi-layer, tri-layer, tetra-layer, and penta-layer MoS_2 slabs were made from the optimized bulk structures and it is again relaxed with the DFT approximation. The optimized structures are shown in the Fig 1(b-f).

After geometry optimization and static calculation, we have studied the band structure of the MoS_2 and plot the band structure along the Γ–M–K–Γ path using the relaxed lattice parameters, as represented in the right side of the Fig 2. The van der Waals interaction were present for all the structures expect for the monolayered one. Our calculated value of the indirect bandgap is found to be 0.94 eV for bulk MoS_2 which is in agreement with the experimental bandgap. [19] For the monolayered nanosheet the direct bandgap of 1.83 eV is found. The reported value of experimental bandgap for the mono-layer structure is ~1.90 eV.[20] For bilayer, tri layer, tetra layers and penta layered structures, the bandgap is indirect and the value is 1.24 eV, 1.05 eV, 0.68 eV and 0.00 eV, respectively. The experimental indirect band gap for double layer MoS_2 structure is ~1.26 eV[21] and tri-layer is ~1.20 eV[19] according to earlier published works. Our calculated values of bandgap are in close agreement with available experimental results. The density of states (DOS) for all these structures are shown in the left panel of Fig 2. It is shown that DOS is symmetric for both spin up and spin down atoms. This indicates that MoS_2 nanosheets are non-magnetic. The bandgap is decreasing with the increasing of number of layers in the structures. For the case of five layered and more the semiconducting MoS_2 showed metallic behavior, which is not consistent with other calculations and experimental findings. This disagreement is due to the van der Waals force we incorporated among the layers in our theoretical calculations. This may be due to the effectiveness of the large van der Waals force between the layers. It is clear from the Fig 2 that with the increasing the number of layers the valance band maxima is shifting from the K points towards the Γ point, and the conduction band minima is moving to the opposite direction. This shifting of conduction and valance band edge may have significant effect on the optical absorption of the MoS_2 nanosheet.

As the number of layers of MoS_2 increases, the band gap monotonically decreases.[22] MoS_2 nanosheets have radically different properties compared to the bulk system. For finite number of layers, the interlayer van der Waals interactions is being removed, the itinerant electrons get confined due to the finite size effect of the nanosheet which leads to the direct bandgap as contrary to the bulk MoS_2. The indirect to direct transition of the bandgap is shown in the Fig 3, which is consistent with the previous calculations. [23,20] Direct band gap in two-dimensional transition metal dichalcogenides depends on the localized d orbital of transition metal, and due to the location in the unit cell, these are slightly affected by the interlayer coupling. But the indirect bandgap depends on the overlap of d orbital of transition metal and p_z orbital of chalcogenide atoms which depends on the interlayer coupling. Bulk and multi-layered structures are found to have indirect bandgap whereas monolayer structure has a direct bandgap.

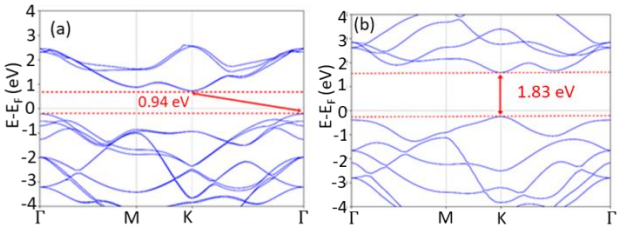

Fig. 3. Transition from indirect to direct bandgap of (a) bulk and (b) monolayer of MoS_2

As we moved from the monolayer to bi-layer, tri-layers, and tetra-layers MoS_2 nanosheets, the direct bandgap again converted to indirect bandgap like the bulk MoS_2. This is due to the reason of van der Waals interaction between the layers, which was absent for the mono layer MoS_2 nanosheet. The quantum confinement of electrons in the monolayer MoS_2 make this nanosheet suitable for catalytic applications, and the bandgap of layered MoS_2 is suitable for photovoltaic applications. The band gap of the bulk and up to five layers of MoS_2 nanosheets are summarized in Table 1.

Table 1. The conduction band minima (CBM), valance band maxima (VBM), value of band gap, and direct or indirect nature of band gap.

Number of layers	CBM (eV)	VBM (eV)	Band Gap (eV)	Nature of Band Gap
1	1.58	-0.25	1.83	Direct
2	1.03	-0.21	1.24	Indirect
3	0.82	-0.23	1.05	Indirect
4	0.45	-0.24	0.68	Indirect
5	0.40	-0.04	0.45	Indirect
Bulk	0.72	-0.22	0.94	Indirect

STM Simulation of MoS_2 Surface

It is a long-standing debate whether the MoS_2 surface is terminated by S atoms or by Mo atom because the identical structure of S and Mo surface lattice.[24–27] To observe the surface termination and morphology of clean MoS_2 1X1 surface, we have applied the Tersoff-Hamman approximation[14] to simulate the STM images. The tunneling current I is measured as a function of tip position by the equation 1.

$$I = \sum_{v} |\psi_s|^2 \delta(E_s - E_F) = \rho(r, E_F) \qquad (1)$$

Where E_s is the energy of the s'th Khon-Sham orbital, E_F is the energy of the Fermi level and ψ_s is the wavefunction of the s'th Khon-Sham orbital. The electron density is given by $\rho(r, E_F)$ near the Fermi energy. The electronic density is calculated around the Fermi energy by using the VASP code and plot them in a constant height of the iso-surface to produce the STM image.

In the MoS_2 unit cell the dz^2 orbital of Mo is situated on top of the valance band which may be responsible for the appearance of Mo atoms on the STM images, on the other hand the attenuation of d orbital as compared to the s or p orbital can play role to visualize S atoms rather than Mo atoms in the STM image.[25]. We have used Tersoff-Hamman approximation[14]. there is no direct electronic mixing between the tip atom and surface atom withing this approximation. To do this with the VASP package, we first complete a self-consistence force (scf) calculation of a 1x1 MoS_2 surface, and then we generate the partial charge of the system, once the partial charge is generated, the iso-surface of the charge is plot via the VESTA code, which is basically the STM image of the system. Clean MoS_2 (1x1) surface was scanned using negative bias voltage of -1 V and positive bias voltage of +1 V using three different tips (Tungsten tip, Molybdenum tip) in the constant height mode. Tip apex atom was kept at a fixed height of 4 Å from the top surface atom in all scans. Resulting tunneling current from (to) sample (tip) was recorded.

Fig 4(a) shows the resulting STM image of MoS_2 (1x1) cell using tungsten tip, the left image is for -ve bias potential and the right image in Fig 4(a) is for positive bias potential. In both cases of negative or positive bias potential. In the case of molybdenum tip with –ve bias Fig 4(b) and sulfur tip with both positive and negative bias Fig 4(c) Sulphur atom are being seen in the STM image. In the case of molybdenum tip with +ve bias, molybdenum atom is being imaged.

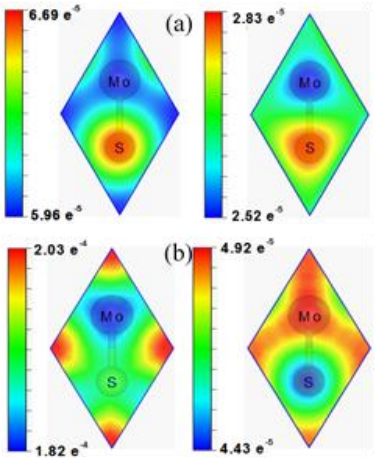

Fig. 4. STM images of 1x1 MoS_2 with (a) Tungsten tip. Left is with –ve bias potential, and right is with +ve bias potential, (b) Molybdenum tip. Left is with –ve bias potential, and right is with +ve bias potential.

To understand the STM image presented in Fig 4, we have calculated the projected density of states (PDOS) of both the tip atoms and the surface atoms of MoS_2 as presented in the Fig 5(a) and Fig 5(b) respectively. The total DOS for all the three tips have very large DOS near the Fermi level as seen in Fig 5(a). For the W tip the d_{xz} orbital large density near the Fermi level in the unoccupied states. This is the conduction band minima of the W atom, this d_{xz} orbital will contribute to the image formation when scanned the MoS_2 surface, and the greater contributing orbital for the case of Mo tip is also d_{xz}, The dz^2 orbital has a peak at an energy around 1.0 eV in the unoccupied side and around -1 eV energy in the occupied side. This orbital may contribute to the STM images for the case of 1.0 eV potential in either positive or negative bias. For the case

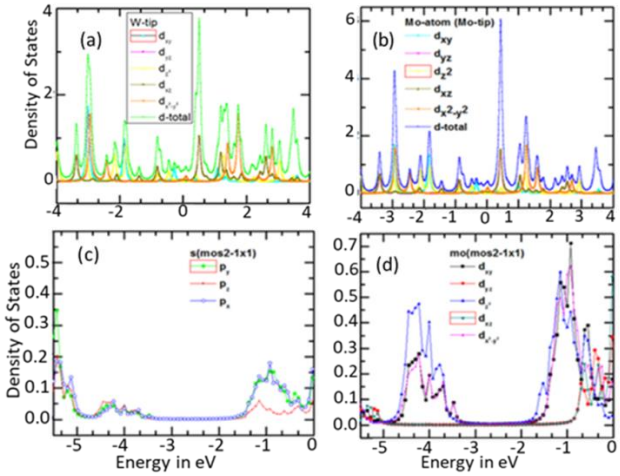

Fig. 5. The orbital projected density of states of the (a) W- tip, (b) Mo-tip, (c) S atom on the MoS_2 surface, and (d) Mo atom on the MoS_2 surface.

Of MoS_2 surface the p_y orbital of S atom is dominant at the Fermi level and d_z^2 orbital of Mo is dominant at the Fermi level. All the other orbitals are very deep in energy so does not have any probability to contribute for the bias potential of 1 eV. We have used 1 eV of biasing potential for both the positive and negative bias case. In all the cases the S atom is visible in the STM images as summarized in Table 1, this because of the interaction of S atoms p orbital with dxz orbital of W tip atom and dz^2 orbital of Mo tip atom.

Table 2. Type of atom imaged with respect to type of tip atoms and nature of applied bias potential

Tip Atom	Negative bias	Positive bias
Tungsten (W)	S	S
Molybdenum (Mo)	S	Mo

IV. Conclusions

The structural and electronic properties of MoS_2 nanosheets of various sizes, shapes, and geometries have been studied. The electronic structure studies of monolayer, bilayer, trilayer, tetralayer and pentalayer have been performed. The bandgap of the bulk MoS_2 is found to be 0.94 eV, which is consistent with other studies. The bandgap of the layered nanosheets are increasing as the number of layers are increasing. The maximum obtained gap is 1.80 eV for the monolayer MoS_2 nanosheet. There is indirect to direct transition of band gap from bulk to mono layer of MoS_2. The simulated STM images showed that sulfur atoms have larger electronic density near Fermi level since they are clearly imaged under STM. The symmetric DOS and PDOS

of these structures indicate the non-magnetic nature of these MoS_2.

References

1. Gu, W., J. Shen, and X. Ma, 2014. Fabrication and electrical properties of MoS 2 nanodisc-based back-gated field effect transistors. *Nanoscale Res. Lett.* **9**, 100.
2. Klinovaja, J. and D. Loss, 2013. Spintronics in MoS 2 monolayer quantum wires. *Phys. Rev. B* **88**, 75404.
3. Eijsbouts, S., 2009. Hydrotreating Catalysts. *Synth. Solid Catal.* 301–328. doi:10.1002/9783527626854.ch14.
4. Chhowalla, M. and G. A. J. Amaratunga, 2000. Thin films of fullerene-like MoS 2 nanoparticles with ultra-low friction and wear. *Nature* **407**, 164–167.
5. Min, S. and G. Lu, 2012. Sites for high efficient photocatalytic hydrogen evolution on a limited-layered MoS2 cocatalyst confined on graphene sheets—the role of graphene. *J. Phys. Chem. C* **116**, 25415–25424.
6. Geim, A. K. and I. V. Grigorieva, 2013. Van der Waals heterostructures. *Nature* **499**, 419–425.
7. David, L., R. Bhandavat, and G. Singh, 2014. MoS2/graphene composite paper for sodium-ion battery electrodes. *ACS Nano* **8**, 1759–1770.
8. Chang, K. and W. Chen, 2011. L-cysteine-assisted synthesis of layered MoS2/graphene composites with excellent electrochemical performances for lithium ion batteries. *ACS Nano* **5**, 4720–4728.
9. Rai, D. P., V. Vu. Tuan, L. Amel, M. P. Ghimire, P. K. Patra, and S. Sunita,2019. Electronic and optical properties of 2D monolayer (ML) MoS2 with vacancy defect at S sites. *Nano-Structures and Nano-Objects* 100404. doi:10.1016/j.nanoso.2019.100404.
10. Chhowalla, M., Z. Liu, and H. Zhang, 2015. Two-dimensional transition metal dichalcogenide (TMD) nanosheets. *Chem. Soc. Rev.* **44**, 2584–2586.
11. Zhou, W. Z. Xiaolong, N. Sina, L. Zhen, S. Yumeng, K. Jing, L. Jun, M. A. Ajayan, I. Y. Boris, and I. Juan, 2013 Intrinsic structural defects in monolayer MoS2. *Nano Lett.* **6**, 2615–2622.
12. Splendiani, A., L. Sun, Y. Zhang, T. Li, J. Kim, C. -Y. Chim, G. Galli, and F. Wang, 2010 Emerging photoluminescence in monolayer MoS 2. *Nano Lett.* **10**, 1271–1275.
13. Li, T. and G. Galli, 2007. Electronic properties of MoS2 nanoparticles. *J. Phys. Chem. C* **111**, 16192–16196.
14. Tersoff, J. and D. R. Hamann, D. R. Theory of the scanning tunneling microscope. *Phys. Rev. B* **31**, 805.
15. Kresse, G. and J. Furhmuller, 1993. Software VASP, Vienna (1999); Kresse G. and Hafner. *Phys. Rev. B* **47**, R558.
16. Perdew, J. P., 1997. Phys. Rev. Lett. 1996, 77, 3865--3868; erratum J. P Perdew, K. Burke, M. Ernzerhof. *Phys. Rev. Lett* **78**, 6.
17. Böker, T., R. Severin, A. Muller, C. Janowitz, R. Manzke, D. Vob, P. Kruger, A. Mazur, and J. Pollmann, 2001. Band structure of MoS 2, MoSe 2, and $α$- MoTe 2: Angle-resolved photoelectron spectroscopy and ab initio calculations. *Phys. Rev. B* **64**, 235305.
18. Bollinger, M. V, K. W. Jacobsen, and J. K. Nørskov, 2003. Atomic and electronic structure of MoS 2 nanoparticles. *Phys. Rev. B* **67**, 85410.
19. Ahmad, S. and S. A. Mukherjee, 2014. comparative study of electronic properties of bulk MoS2 and its monolayer using DFT technique: application of mechanical strain on MoS2 monolayer.
20. Mak, K. F., C. Lee, J. Hone, J. Shan, and T. F. Heinz, 2010. Atomically thin MoS 2: a new direct-gap semiconductor. *Phys. Rev. Lett.* **105**, 136805.
21. Rahman, I. A. and A. Purqon, 2017. First Principles Study of Molybdenum Disulfide Electronic Structure. *J. Phys. Conf. Ser.* **877**.
22. Laurencin, C. T. and R. James, 2014. Composites and structures for regenerative engineering. *J. Fluid Mech.* **1621**.
23. Piper, J. R. and S. Fan, 2016. Broadband absorption enhancement in solar cells with an atomically thin active layer. *Acs Photonics* **3**, 571–577.
24. Fisher, A. J. and P. E. Blöchl, 1993. Adsorption and scanning-tunneling-microscope imaging of benzene on graphite and MoS 2. *Phys. Rev. Lett.* **70**, 3263.
25. Magonov, S. N. and M. H. Whangbo, 1994. Interpreting STM and AFM images. *Adv. Mater.* **6**, 355–371.
26. Weimer, M., J. Kramar, C. Bai, and J. D. Baldeschwieler, 1988. Tunneling microscopy of 2H-MoS 2: A compound semiconductor surface. *Phys. Rev. B* **37**, 4292.
27. Whangbo, M.-H., J. Ren, S. N. Magonov, H. Bengel, B. A. Parkinson, and A. Suna, 1995. On the correlation between the scanning tunneling microscopy image imperfections and point defects of layered chalcogenides 2H MX2 (M= Mo, W; X= S, Se). *Surf. Sci.* **326**, 311–326.